Solar Phys (2007) 242: 53–63
DOI 10.1007/s11207-007-0213-y

Observation of Interactions and Eruptions of Two Filaments

Jiangtao Su · Yu Liu · Hiroki Kurokawa · Xinjie Mao · Shangbin Yang · Hongqi Zhang · Haimin Wang

Received: 28 April 2006 / Accepted: 6 June 2007 / Published online: 13 July 2007

Abstract We present new observations of the interactions of two close, but distinct, Hα filaments and their successive eruptions on 5 November 1998. The magnetic fields of the filaments are both of the sinistral type. The interactions between the two filaments were initiated mainly by an active filament of one of them. Before the filament eruptions, two dark plasma ejections and chromospheric brightenings were observed. They indicate that possible magnetic reconnection had occurred between the two filaments. During the first filament eruption, salient dark mass motions transferring from the left erupting filament into the right one were observed. The right filament erupted 40 minutes later. This second filament eruption may have been the result of a loss of stability owing to the sudden mass injection from the left filament. Based on the Hα observations, we have created a sketch for understanding the interactions between two filaments and accompanying activities. The traditional theory of filament merger requires that the filaments share the same filament channel and that the reconnection occurs between the two heads, as simulated by DeVore, Antiochos, and

Electronic Supplementary Material The online version of this article (http://dx.doi.org/10.1007/s11207-007-0213-y) contains supplementary material, which is available to authorized users.

J. Su (✉) · S. Yang · H. Zhang
National Astronomical Observatories, Chinese Academy of Sciences, Beijing 100012, China
e-mail: sjt@bao.ac.cn

Y. Liu
Institute for Astronomy, University of Hawaii, 2680 Woodlawn Drive, Honolulu, HI 96822, USA
e-mail: lyu@ifa.hawaii.edu

H. Kurokawa
Kwasan and Hida Observatories, Kyoto University, Yamashina-Ku, Kyoto 607-8471, Japan

X. Mao
Astronomy Department, Beijing Normal University, Beijing 100875, China

H. Wang
Center for Solar-Terrestrial Research, New Jersey Institute of Technology, University Heights, Newark, NJ 07102, USA

Aulanier (*Astrophys. J.* **629**, 1122, 2005; **646**, 1349, 2006). Our interpretation is that the external bodily magnetic reconnection between flux ropes of the same chirality is another possible way for two filament bodies to coalesce.

Keywords Filaments · Activities

1. Introduction

Solar prominences or filaments consist of cold dense plasma suspended in the corona. Filaments are observed to form and exist in filament channels – a magnetic environment in which a filament can be supported by the magnetic field of a helical flux rope. It is known that a pair of filaments that are closely located on the solar disk sometimes approach each other and interact (d'Azambuja and d'Azambuja, 1948). Under favorable conditions, two filaments with the same chirality can link up to form a single and larger filament (*e.g.*, Deng *et al.*, 2000). In contrast, two filaments with different chirality are usually observed to avoid each other and retain their distinct identities (*e.g.*, Schmieder *et al.*, 2004). These empirical rules for filament interactions have been confirmed by detailed numerical simulations of interacting filaments (DeVore, Antiochos, and Aulanier, 2005, 2006). The rules of chiralities seem to also work for other solar activity, as indicated by the observational evidence for sunspots and filament barb disintegrations (Liu and Zhang, 2002; Liu *et al.*, 2007; Su *et al.*, 2005). Based on 3D numerical simulations, Linton, Dahlburg, and Antiochos (2001) have demonstrated how counter-helical fluxes reconnect to release the nonpotential energy of a magnetic field. It should be noted that Linton's simulation applies in the convective zone with confined flux tubes with high plasma β, and it is unclear whether the same physics is applicable in the solar corona.

Observations of interacting filaments are valuable and can contribute to verifying different filament models and to a better understanding of the coronal magnetic field structures as well as the coronal dynamics. However, observational reports on them are rare. Using the data taken with solar radio telescopes, Uralov *et al.* (2002) argued that a coronal mass ejection (CME) on 4 September 2000 was initiated in a dual-filament system. In this event, the merger process of the two filaments was thought to have caused the subsequent opening of the coronal fields to release a CME. Their observational conclusion is attractive, but the details of the filament merger in the event are very limited because of the lack of simultaneous Hα data.

We occasionally found a well-observed case showing the interaction between two filaments associated with their eruptions when searching for solar surges with the automatic detection method developed by Liu *et al.* (2005). Different from those filament mergers with head-to-head linking, the two filaments in the event are found to be united by external bodily reconnections. The magnetic reconnection between the two magnetic ropes could play an important role in transferring material from one filament into the other and, consequently, destroying their stability. Su *et al.* (2005) have discussed the first filament eruption and found that it had a close relation to the helicity reversal in the magnetic flux on the photosphere that was revealed from the evolution of one filament barb. This is a follow-up paper to further study the interaction between the two filaments.

2. Observations and Data Analysis

2.1. Data

The full-disk Hα observations were made at the Hida Observatory with the Flare Monitoring Telescope (FMT) (Kurokawa *et al.*, 1995) and Big Bear Solar Observatory (BBSO). The

FMT can simultaneously supply three Hα images at (Hα center, ±0.8 Å) with a temporal cadence of two seconds and a spatial resolution of 4″ pixel^{-1}. The Hα images provided by BBSO are of a high spatial resolution of 0.6″ pixel^{-1}. They are used to analyze the activity of the two filaments. The images taken by SOHO/EIT (λ 195 Å; Delaboudiniere *et al.*, 1995) with an average cadence of 12 minutes are available for the analysis of filament eruptions observed in the EUV wavelength. The SOHO/MDI (Scherrer *et al.*, 1995) full-disk magnetograms are used to study the magnetic fields of the filaments.

The FMT Hα data have been improved by enhancing the image contrast through subtraction of the quiet Sun's center-to-limb variation profile. All of the full-disk data taken at different times have been co-aligned based on the nonlinear mapping, which takes into account the solar differential rotation (Chae *et al.*, 2001).

2.2. Observations of the Filaments During 3 – 6 November 1998

Figure 1 shows the daily development of the filaments using BBSO Hα images taken during 3 – 6 November 1998. In Figure 1a, the left filament appears as a ∪ shape; *i.e.*, it is highly curved. The filaments were located close together in a decayed active region at S28 in the southern hemisphere during the observations. The obvious contrast differences among the frames in Figure 1 are due to the changing seeing conditions. With good seeing conditions on 4 November, the outline of the filament channel, indicated by an arrow in Figure 1b, turned out to be clear in the data, and the northern part of the right filament had developed in a more integrated formation (Figure 1b). Interestingly, this location between the two arrows is also the site where two surge-like ejections occurred on 4 November 1998. They will be analyzed in Section 2.3.

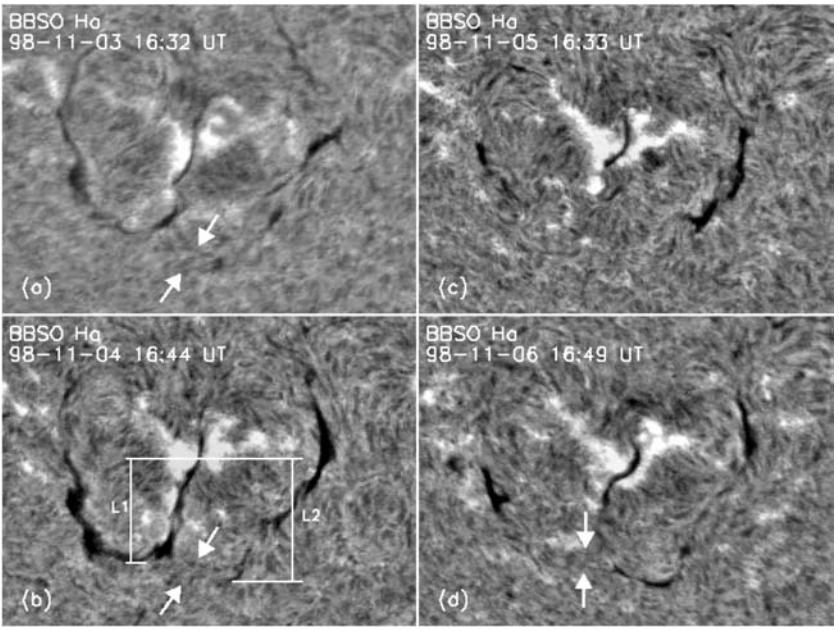

Figure 1 Development of the two filaments during four days (3 – 6 November 1998). The white arrows point to the locations of the filament channels. The field of view of the Hα images is 400″ × 300″. Solar North is to the top and West to the right in this and all of the following figures.

On 5 November, between 01:31 and 02:38 UT, the left and right filaments erupted successively. The eruptions were observed by the FMT instrument. The eruption of the right filament will be described in Section 2.4. The time interval between the two eruptions is no more than 40 minutes. Figure 1c is a BBSO image taken after the filament eruptions. In this image, we can see that the right filament clearly reappeared after its eruption, whereas the left filament was much weaker after its eruption.

On the following day (Figure 1d), the left filament remained fragile and faint, but the right filament had formed a well-defined ∪ shape that may have resulted from the material filling from the filament channel. The two arrows in Figure 1d show the empty part of filament channel.

From the description of Figure 1, one can see that the two filaments had exchanged their appearances from 3 to 6 November; that is, the left filament channel lost a great deal of cool material while the right one gained significant cool material.

The reason for the growing filament on the right side after the eruption is unclear owing to the limitations of our data. It may be due to the direct transfer of the material from the old, left filament after the merger, or to chromospheric injections from below by converging magnetic polarities, or to both. Liu, Kurokawa, and Shibata (2005) have demonstrated several observational cases showing that chromospheric mass injection is an effective way to form an observable Hα filament. However, Wang *et al.* (2001) find a special surge ejection from the end of an erupted filament. Nonetheless, this problem is beyond the scope of this paper, which focuses on the interaction between the two filaments and their eruptions.

The lower parts of the two filaments (channels) are denoted with white lines in Figure 1b. The projection gap between them appears to be shortened on 4 November. In Figure 1b, L1 and L2 are the distances from the center of the magnetic cancellation region (corresponding to the Hα brightening) to the filament bottoms, respectively. Figure 2 is a plot of L1 – L2 from 16:53 UT to 22:23 UT on 4 November. That the difference between L1 and L2 gradually reaches zero implies that the two filaments were approaching each other. The average approaching velocity is 10.0 m s^{-1}, and the average acceleration is 3.9 m s^{-2}. Furthermore,

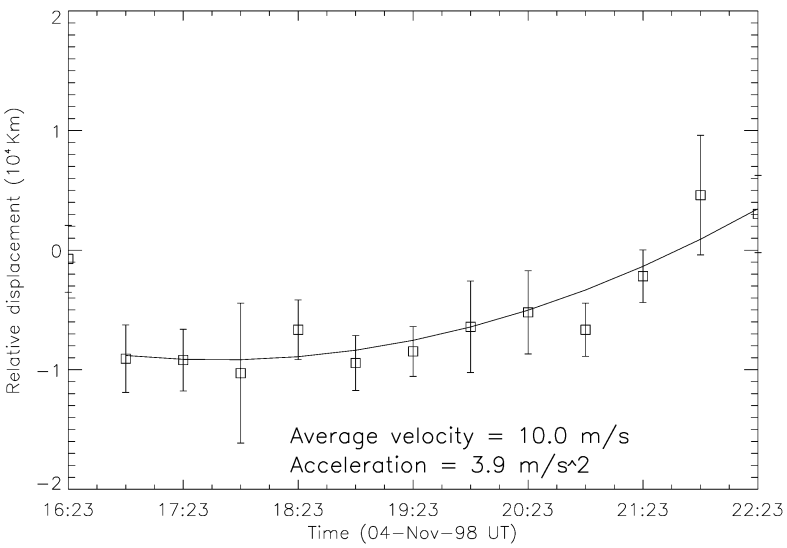

Figure 2 The relative displacement in the *y*-direction between L1 and L2 in panel (b) of Figure 1.

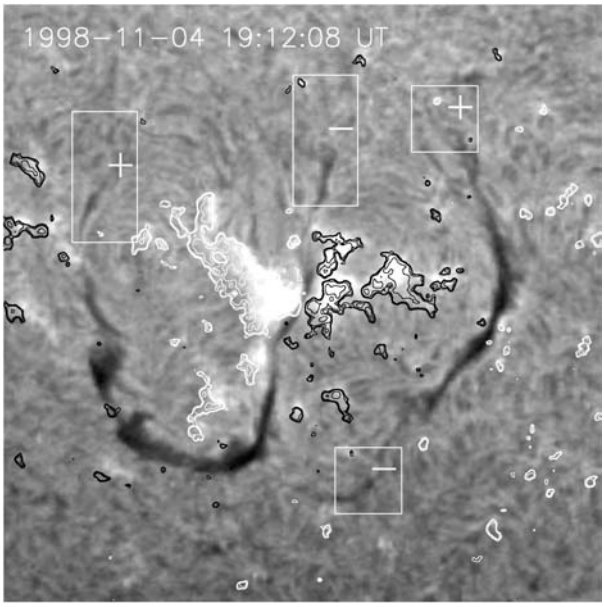

Figure 3 A BBSO Hα image overlaid with an MDI magnetogram. The size of the field of view is $360'' \times 360''$. The white (black) contours show positive (negative) magnetic polarities.

this approaching motion could have led to the compression between the two magnetic flux ropes of the filaments in the West – East direction. The idea that the continual impact might have driven the magnetic reconnection or merger between them needs to be confirmed by future numerical simulations.

Figure 3 is an example of an Hα image overlaid with the contours of the MDI magnetogram. The ∪-like filament represents a highly-twisted flux rope that is often observed as an SXR sigmoid configuration in the solar corona (Canfield, Hudson, and McKenzie, 1999). After using the local-correlation-tracking method (Chae *et al.*, 2001), we obtained the proper motion velocities of the main positive and negative flux. At about 16:06 UT, the average velocity of the positive flux is 0.34 km s^{-1}, and that of the negative flux is 0.21 km s^{-1}. We think the penetration between them should not be ignored because it is a condition favorable for driving magnetic reconnections. The persistent Hα brightening patches indicate the location of the magnetic reconnections. Based on the comparison of Hα data with simultaneous MDI magnetic-flux contours, the magnetic chiralities of the filaments can be easily determined (Martin, Marquette, and Bilimoria, 1992). The signs of polarities for the magnetic fluxes are marked in this figure at the places where the filaments end. In general, they are both in sinistral fields and are consistent with the statistical chirality for filaments in the southern hemisphere.

2.3. Features of Brightening Patches and Surge-like Ejections

In Section 2.2, we have shown evidence for the approaching motions of the two sinistral filaments. Associated with these motions, several Hα brightenings are observed and these extend along the magnetic neutral line, and two subsequent dark surge-like ejections are found at the terminal sites (*i.e.*, Region C in Figure 4) where the two filament channels join. The first cool Hα plasma ejection is referred to as Event 1, and the second as Event 2. In Figure 4, Regions A, B, and C in the white boxes are the three main brightening areas. Obvious downward plasma motions took place in the three boxed regions. For Event 1, the

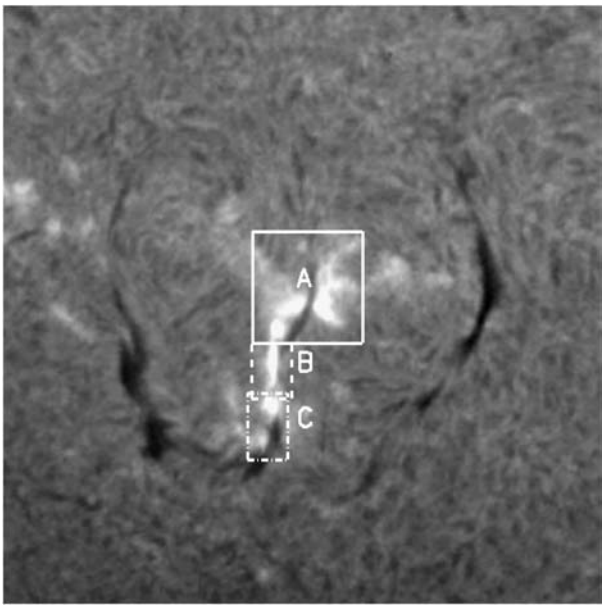

Figure 4 Three boxes that contain the brightening regions, indicated by A, B, and C, shown in a BBSO Hα image.

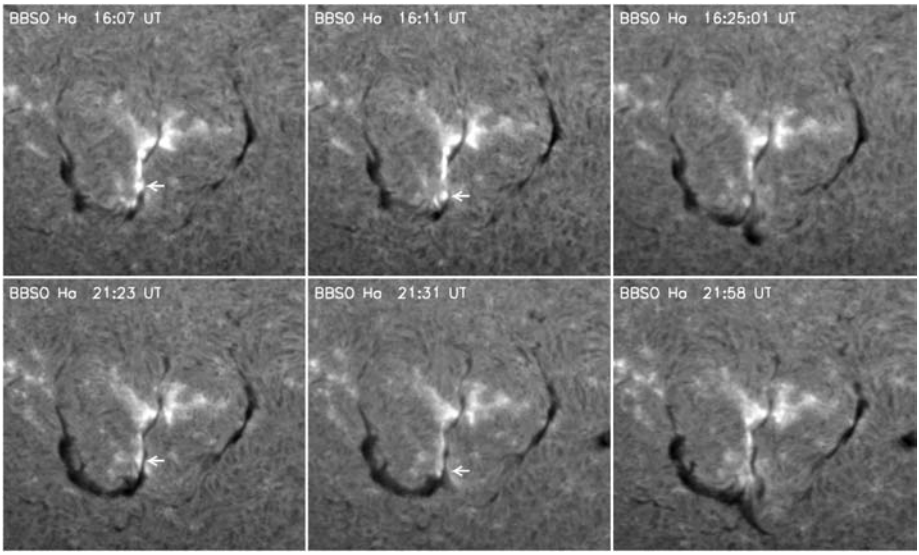

Figure 5 The filament expansions and surge-like ejections observed on 4 November. The white arrows point to the small moving bright dot (in the upper row) and bright-ribbon (in the lower row). The field of view of these Hα images is $400'' \times 360''$.

brightening in Region C is a small compact circle-dot area with a radius of $5.5''$. However, for Event 2, the brightening patch is more diffusive with a width of about $6''$. At the bottom of Region C, the right filament channel obviously joins the left filament body.

Figure 5 shows the temporal sequence of two events observed in the Hα wavelength. The first row is for Event 1, and the second for Event 2. The white arrows point to the

Table 1 Parameters of the two events.

	Motions of brightening patches			Surge-like ejections		
Event	Duration (UT)	v[a] (km s^{-1})	a[b] (km s^{-1})	Duration (UT)	v[a] (km s^{-1})	l[c] (km)
1	16:06 – 16:12	−21.8	−0.012	16:25:16:31	61	180.000
2	21:23 – 21:29	−18.6	−0.662	21:42:22:05	76	330.000

[a]Average projection speed of the Hα brightenings. Note that negative is southward.

[b]Average projection acceleration of the Hα brightenings.

[c]Maximum projection length of the surge-like plasma ejections.

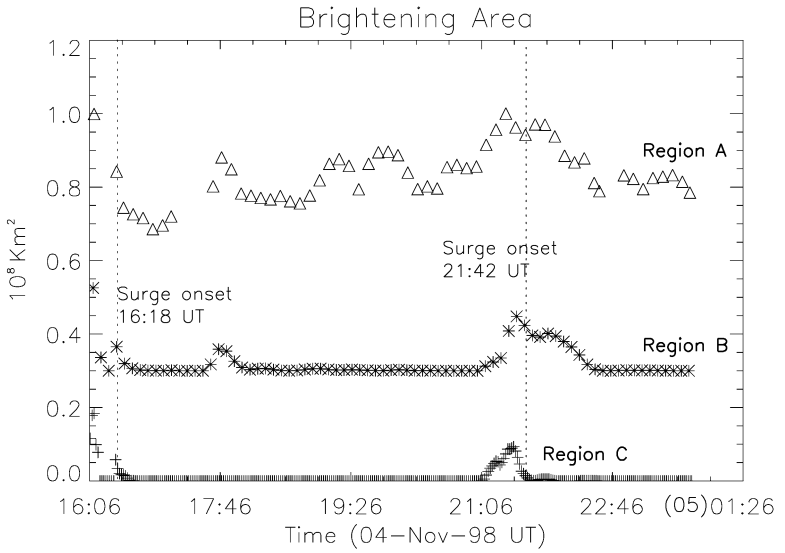

Figure 6 The evolution of the brightening areas of A, B, and C as a function of time in the three boxes in Figure 5. The area of B is increased by 0.3 to better see the curves of B and C.

moving brightening patches. Fresh dark Hα ejections are clearly seen from the end of the touching edge between the two filaments. For Event 1 the average velocity component in the north – south direction of the brightening center in Region C is −21.8 km s^{-1}, with an associated acceleration of 0.012 km s^{-2}; for Event 2 the average velocity component is −18.6 km s^{-1} with an acceleration of 0.662 km s^{-2}. The average projection velocities for the dark surging plasma are 61 km s^{-1} and 76 km s^{-1} for Events 1 and 2, respectively. It seems that the larger the acceleration of the brightening movement, the larger the ejection velocity for Hα surging plasma is. Table 1 presents the parameters for the two events. The surge-like activities might be directly associated with the magnetic reconnections in Region C. Unfortunately, the magnetic field data cannot show the magnetic flux cancellation for this region because of its low resolution.

The plots in Figure 6 show the evolution of the areas for the three brightening regions with time. The vertical dashed lines mark the onsets of the two local plasma ejections (16:18 UT and 21:42 UT). The starting times of the surge-like ejections are about 12 and 36 minutes

later than the time of the maximum brightening at the footpoint, respectively. The area values are calculated through a numerical method that counts all the newly darkened pixels in the data. The three brightening areas reached their maximum almost at the same time based on the one-minute cadence data. Additionally, another peak in the profiles is found for both Regions A and B at 17:46 UT. However, there is no such peak found for Region C, and there are no surge-like ejections observed around this peak time.

Although the two Hα ejections took place in Region C, we cannot exclude the possibility that the energy contributions for plasma accelerations were supplied from Regions B and C. This is beyond the scope of this paper.

2.4. Filament Eruptions and Filament Material Transfer

It has been pointed out that, in a flare event, the apparent motions of flare loops and ribbons are not caused by mass transportation of the plasma but by the continual propagation of an energy source into new field lines (*e.g.*, Schmieder *et al.*, 1987). Based on this, we speculate that the initial filament expansion is caused by the increasing pressure of the gas inside the filament heated by the energy released in the reconnection processes in the low atmosphere. The magnetic reconnections can be indicated by the bright moving ribbons along the magnetic neutral line.

The left two columns of Figure 7, including FMT Hα center and Hα-blue-wing observations, show the partial eruption of the left filament on 5 November. There are no obvious flare ribbons observed in the FMT data during this eruption. Su *et al.* (2005) have found a formation of flux with opposite-sign helicity in part of the filament. The white arrows point to the right part of the left filament. In the eruption phase, the right part of the left filament exhibits a clear shape in the Hα-center wavelength, but it shows a very faint shape in the Hα-blueshift wavelength. This implies that although the right part of the left filament was still kept in the chromosphere and disturbed by the left eruption; it did not erupt with the left part.

Interestingly, after the eruption of the material from the left part, the material of the right part of the left filament was observed injecting into the channel of the right filament. The Hα images in the middle column show that the right part of the left filament curved toward

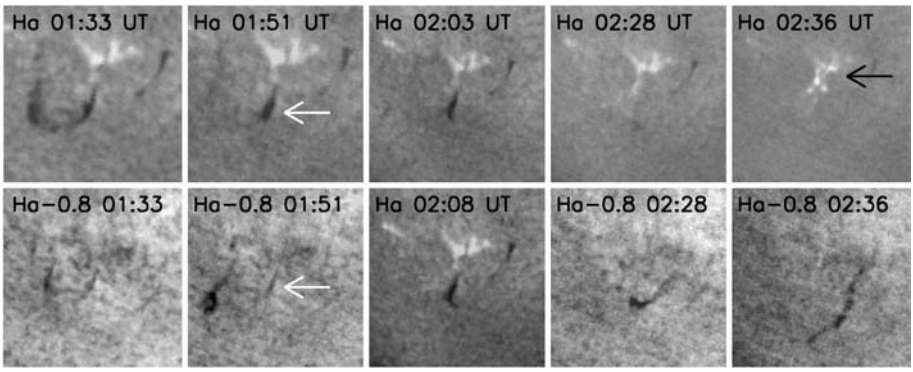

Figure 7 Hida/FMT observations during 01 – 03 UT on 5 November 1998 for the two successive filament eruptions. The left two columns and the right two columns show the first and the second filament eruption, respectively. The purpose of the middle column is to show the injection of mass from the left erupted filament into the right one. The arrows in the second column point to the right part of the left filament. The black arrow in the last column marks the positions of new flare ribbons.

the right filament. For a better demonstration of the complex eruptions, we have made the FMT Hα data into a movie available as additional electronic material with this paper. The movie confirms that the material of the right part of the left filament was really injected into the right filament after the first eruption. Therefore, a new ∪-shaped filament could be generated when the filament channel was transiently filled by the material coming from the left filament. This new filament erupted at about 02:28 UT. Both of the filament eruptions can be seen in the EIT 195 Å observations.

3. Discussion and Conclusions

We conclude from our data that two conditions are necessary for material transfer from one filament to another: (*i*) The flux ropes of the two filaments have the same-sign magnetic chirality and (*ii*) interactions between the two filaments must form a common part of a filament channel to facilitate the mass transfer.

We sum up the important observational features as follows: *i*) The two filaments were originally located close to each other and both were of the sinistral type. *ii*) The left filament slowly approached the right one. *iii*) There were two surge-like plasma ejections near the common border of the two filaments. *iv*) The left part of the left filament erupted first, and its right part merged with the right filament. *v*) The right filament then lost its original balance, and a second filament eruption occurred.

Based on the observations, we present in Figure 8a a simplified model for the interactions of two sinistral filaments. In Figure 8a, the two sinistral filament channels approach each other as the left filament expands. The enlarged dashed box in Figure 8a, displayed in Figures 8b and 8c, shows the twisted ropes. The magnetic reconnection in the θ-direction occurs between the two ropes (Figure 8c). The small brightening areas observed appear in the merging regions, so that it is easy to understand why surge-like ejections were found between the two filaments. Figure 8d shows the configuration of the new filament channel after the merger of the two filaments.

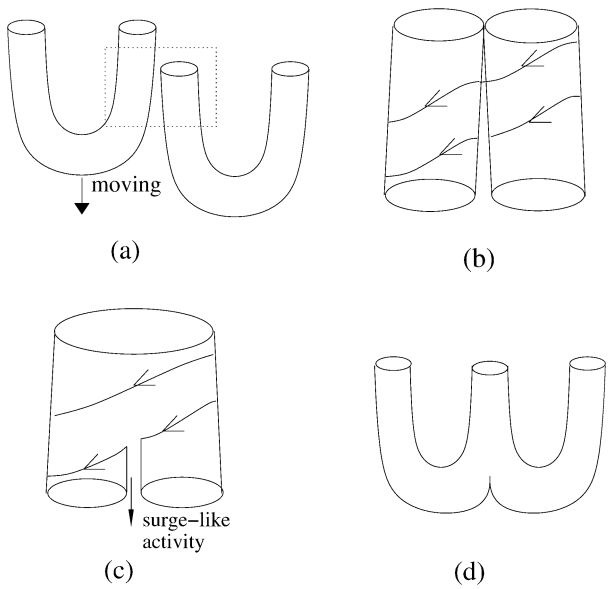

Figure 8 Cartoons explaining the development of the interactions of two sinistral filament channels. The θ-direction reconnections would occur as they approach each other.

From our data, we inferred that the first filament eruption was driven by opposite-sign helical magnetic flux that emerged from below, which has been discussed in the previous paper (Su *et al.*, 2005). The low-layer magnetic reconnection driven by emerging flux that caused the first eruption can be understood by using the tether-cutting model for filament eruptions and flares (Moore *et al.*, 2001). We think that the second filament eruption was caused by just the material injection. A significant question related to the new ∪-like filament (see Figure 1d, at the right) is to examine the possible formation mechanism in it. We think it formed by the interaction of the two tubes because of converging magnetic polarities. Although some observations showed that direct chromospherical material injection is an effective way to form new filaments in a short time scale (Liu, Kurokawa, and Shibata, 2005), the filament formation studied here would not favor this formation mechanism. The new ∪-like filament formation must have a close relation to the interaction between the two old filaments. The first filament eruption has an obvious magnetic-triggering mechanism, whereas the second one seems to have resulted from an overload of mass injected suddenly from the first filament via the common filament channel formed by the filament mergers. However, the magnetic reconnections should have played a crucial role for both the erupting processes. More detailed information about the process is expected from future numerical simulations designed for filament interactions. It has been demonstrated how counter-helical fluxes and identical-helical fluxes reconnect and release the nonpotential energy by Linton, Dahlburg, and Antiochos (2001). We expect to clearly determine whether the same physics is applicable in the solar corona for filament interactions, since Linton's simulation applies in the convective zone with confined flux tubes in plasma with high β.

Acknowledgements We thank L.H. Good, the editor of the *IfA Newsletter* of the University of Hawaii, for the significant improvement of the manuscript. The authors are indebted to Dr. V. Yurchyshyn for providing BBSO Hα data. We would like to thank the staff of SOHO for the MDI and EIT data available from the Internet. SOHO is a project of international cooperation between ESA and NASA. The research of Y. Liu is supported by NSF Grant No. ATM-04-21582. This work is also supported by NSFC Project Nos. 10611120338, 10673016, 60673158, 10473016, and 10273002 and by NBRP Project No. 2006CB806301.

References

Canfield, R.C., Hudson, H.S., McKenzie, D.E.: 1999, *Geophys. Res. Lett.* **26**, 627.
Chae, J., Wang, H., Qiu, J., Goode, P.R., Strous, L., Yun, H.S.: 2001, *Astrophys. J.* **560**, 476.
d'Azambuja, L., d'Azambuja, M.: 1948, *Ann. Obs. Paris Meudon* **6**, 7.
Delaboudiniere, J.-P., *et al.*: 1995, *Solar Phys.* **162**, 291.
Deng, Y.Y., Schmieder, B., Engvold, O., DeLuca, E., Golub, L.: 2000, *Solar Phys.* **195**, 347.
DeVore, C.R., Antiochos, S.K., Aulanier, G.: 2005, *Astrophys. J.* **629**, 1122.
DeVore, C.R., Antiochos, S.K., Aulanier, G.: 2006, *Astrophys. J.* **646**, 1349.
Kurokawa, H., Ishiura, K., Kimura, G., Nakai, Y., Kitai, R., Funakoshi, Y., Shinkawa, T.: 1995, *J. Geomag. Geoelectr.* **47**, 1043.
Linton, M.G., Dahlburg, R.B., Antiochos, S.K.: 2001, *Astrophys. J.* **553**, 905.
Liu, Y., Kurokawa, H., Shibata, K.: 2005, *Astrophys. J.* **631**, L93.
Liu, Y., Kurokawa, H., Kitai, R., Ueno, S., Su, J.: 2005, *Solar Phys.* **228**, 149.
Liu, Y., Kurokawa, H., Liu, C., Brooks, D., Ishii, T., Dun, J., Zhang, H.: 2007, *Solar Phys.* **240**, 253.
Liu, Y., Zhang, H.: 2002, *Astron. Astrophys.* **386**, 646.
Martin, S.F., Marquette, W.H., Bilimoria, R.: 1992, In: Harvey, K. (ed.) *The Solar Cycle*, *ASP Conf. Proc.* **27**, Astronomical Society of the Pacific, San Francisco, 53.
Moore, R.L., Sterling, A.C., Hudson, H.S., Lemen, J.R.: 2001, *Astrophys. J.* **552**, 833.
Scherrer, P.H., *et al.*: 1995, *Solar Phys.* **162**, 129.
Schmieder, B., Forbes, T.G., Malherbe, J.M., Machado, M.E.: 1987, *Astrophys. J.* **317**, 956.
Schmieder, B., Mein, N., Deng, Y., Dumitrache, C., Malherbe, J.-M., Staiger, J., Deluca, E.E.: 2004, *Solar Phys.* **223**, 119.

Su, J., Liu, Y., Zhang, H., Kurokawa, H., Yurchyshyn, V., Shibata, K., Bao, X., Wang, G., Li, C.: 2005, *Astrophys. J.* **630**, L101.
Uralov, A.M., Lesovoi, S.V., Zandanov, V.G., Grechnev, V.V.: 2002, *Solar Phys.* **208**, 69.
Wang, H., Chae, J., Yurchyshyn, V., Yang, G., Steinegger, M., Goode, P.: 2001, *Astrophys. J.* **559**, 1171.